Adsorption of fluids in a pore with chemical heterogeneities: The cooperative effect

Zhikuan Feng,[1,2] Xianren Zhang,[1] and Wenchuan Wang[1]
[1]*Division of Molecular and Materials Simulation, Key Laboratory for Nanomaterials, Ministry of Education, Beijing University of Chemical Technology, Beijing 100029, China*
[2]*College of Science, Beijing University of Chemical Technology, Beijing 100029, China*
(Received 17 January 2008; published 15 May 2008)

In this work, we study the cooperative adsorption of fluids in a heterogeneous pore, in which the pore walls are composed of homogeneous substrates with chemical groups (CGs) decorating them. The adsorption caused by the homogeneous substrates alone and that by CGs do not add up to the overall adsorption, indicating the existence of a cooperative effect. The cooperative effect is the source of cooperative adsorption, and is characterized in this work by the ratio of the overall adsorption to the sum of adsorption by the substrate only and that by CGs. It is found that the cooperative adsorption does not depend monotonically on the substrate or the CGs. Two different origins of the cooperative adsorption play different roles depending on which one dominates the overall adsorption. Our simulations reveal that, when the homogeneous substrate dominates the overall adsorption, weakening of the attractive fluid-substrate interaction or alternatively strengthening of the fluid-CGs interaction leads to a stronger cooperative effect and enhances the cooperative adsorption. However, when CGs dominate the overall adsorption, weakening of the attractive fluid-CG interaction or strengthening the fluid-substrate interaction results in strong cooperative adsorption. In order to investigate the effects of the distribution of CGs on cooperative adsorption, a design-test method is generalized and used in this work. Simulation results show that the overall adsorption can be significantly affected by the CG distribution.

DOI: 10.1103/PhysRevE.77.051603 PACS number(s): 68.43.−h, 68.43.Fg, 68.08.De, 61.46.Fg

I. INTRODUCTION

Organically functionalized mesoporous materials have received substantial attention in their applications in the field of catalysis, sensing, and adsorption. Moreover, decoration of the solid surfaces of porous media to improve the interaction between guest molecules and the pore walls is essential in the synthesis of ordered mesoporous materials with the "hard-template" approach [1]. Several routes for the synthesis of organically functionalized mesoporous silica solids have been proposed in the literature (see, for example, the works by Wight and Davis [2] and Lim *et al.* [3], and references therein). For mesoporous carbon and titanium dioxide nanomaterials, chemical modifications of the interior surfaces are also currently in progress, as recently reviewed by Liang *et al.* [4] and Chen and Mao [5], respectively.

The effects of surface heterogeneities on adsorption behaviors are under extensive investigation due to the wide applications of fluid adsorption in confined spaces. For example, silanol located on the pore walls of mesoporous silicates can attract fluid molecules by participating in the formation of hydrogen bonds with the adsorbed molecules. However, as demonstrated by Jaroniec *et al.* [6], the standard adsorption analysis has limited applicability for characterization of chemically modified porous silica, since it does not account for the energetic and/or geometrical heterogeneity inherent in real porous surfaces. The authors of [6] also showed that low-pressure nitrogen adsorption isotherms are sensitive to the surface changes caused by chemical modification of silica. To correctly evaluate the effects of surface heterogeneities, however, one needs to consider the effects on not only the low-pressure but also the high-pressure parts, in particular, the capillary condensation.

There is a sizable body of theoretical research available devoted to the study of the effects of surface heterogeneity on fluid adsorption (for a recent review, see [2,3]). This encompasses the density functional theory (DFT) [9–20], Ising lattice models [17,21,22], and computer simulation methods [9,23–42]. The effects of chemical heterogeneity have been examined for slits [9–11,13,17,21,23–30,32,33,42], cylindrical pores [9,16,38–41], and disordered pores [12,15,18–20,22,31,34,35,37]. For example, there in general exist two different models for the chemical heterogeneity of the slit pore [7]. In the first case, the pore surface is divided into domains of strongly and weakly attractive regions. For a slit pore with a nanoscopic chemical pattern of a certain symmetry, a new kind of thermodynamic phase, i.e., fluid bridges [8] spanning between the substrates, may appear under suitable conditions. In the second case, individual chemical groups (CGs) are attached to the pore surface. For a surface with chemically different domains, the adsorption behavior depends strongly on the ratio of the domain size to the pore width [7,8]. On the other hand, for a surface decorated by individual CGs, the behavior depends on the site density. When the ratio or site density is sufficiently small, the behavior is qualitatively similar to that for the homogeneous walls, because the effects of surface heterogeneity are negligible. In contrast, when they are large the behavior is similar to that of a collection of independent pores of various sizes or fluid-adsorbate interactions [7]. As pointed out by Gelb *et al.* [7], intermediate cases between these two extremes are of particular interest. For example, in most cases of realistic surfaces, the heterogeneity can be considered as a combination of the homogeneous substrate (surface homogeneities) and chemical heterogeneities decorating it, which affect the adsorption simultaneously and cooperatively. Thus, an important question emerges: How do the homogeneous substrate and the chemical heterogeneities couple or interplay to affect the overall adsorption?

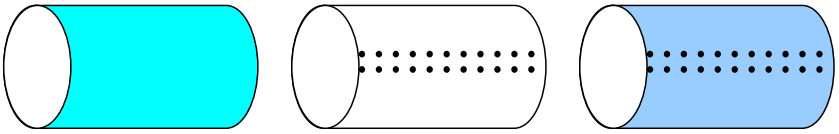

(a) surface I (b) surface II (c) surface III

FIG. 1. (Color online) Sketches for the three pore models. (a) Surface I is an ideal cylindrical pore with an attractive and homogeneous wall. For this model, the interaction potential between a fluid molecule and the wall is described by an analytical function [41] which is integrated over the whole wall surface. (b) Surface II is a hard cylindrical pore with energetic heterogeneities. In this model the energetic heterogeneities are represented by a number of discretely distributed CGs. Except for the fluid-CG interaction represented by the LJ potential, the wall is purely repulsive. (c) Surface III is a pore model with both a homogeneous surface and a number of CGs.

Although there are numerous works on systems with chemical heterogeneity, most of them concentrate on how the overall adsorption is affected by heterogeneities, rather than the interplay between the homogeneous substrate and the chemical heterogeneities. This is to say, to our best knowledge, the interplay has not been thoroughly investigated. As is shown below, the adsorption caused by the homogeneous substrate only and that by the chemical heterogeneity do not necessarily add up to the overall adsorption, which indicates the existence of a cooperative effect. It is the cooperative effect or the interplay that promotes the overall adsorption. For this reason, as a necessary step to characterize organically functionalized mesoporous materials, the present work aims at providing an understanding of the interplay of the substrate and the chemical heterogeneity in the overall adsorption. This is an indispensable prerequisite for characterizing the organically functionalized materials in a second step. The remainder of this paper is organized as follows. In Sec. II, the model and the simulation methods are introduced. In Sec. III, we discuss the corresponding simulation results. In the final section, we summarize the main findings and the relevant conclusions.

II. METHOD AND MODELS

In this work, the grand canonical Monte Carlo (GCMC) method, in which temperature, pore volume, and chemical potential are independent variables, was used to generate adsorption isotherms of fluids in cylindrical pores. Three types of moves were carried out in the GCMC simulation to generate a Markov chain: moving, creating, and deleting a fluid molecule. The heterogeneity in this work is represented by a number of chemical groups on the homogeneous substrate. When we consider the effects of CG distribution on the overall adsorption, the canonical ensemble Monte Carlo (*NVT* MC) method was used. In the *NVT* MC simulations, another type of move, i.e., moving a CG along the solid surface, was introduced to optimize the CG distribution.

To separate the effects of different chemical composition (modeled by the CGs and homogeneous substrate, respectively) on adsorption and then to identify their cooperative effect, three kinds of surface were introduced in this work (see Fig. 1). First, a homogeneous cylindrical pore was adopted to model ideal adsorption of fluid molecules on a homogeneous substrate. In our simulations, the interaction between a fluid molecule and the homogeneous surface is described by following energy function [43]:

$$U(R,l) = \frac{7\pi^2\rho_{\text{solid}}\varepsilon_{\text{sub}-f}}{32}\frac{1}{R^9[1-(l/R)^2]^9} \times F\left[-9/2;-7/2;1;\left(\frac{l}{R}\right)^2\right] - \frac{\pi^2\rho_{\text{solid}}\varepsilon_{\text{sub-}f}}{R^3[1-(l/R)^2]^3}F\left[-3/2;-1/2;1;\left(\frac{l}{R}\right)^2\right], \quad (1)$$

where U is the interaction energy of a fluid molecule at the radial distance l from the center of a cylindrical pore of inner radius R. ρ_{solid} is the number density of solid sites inside the pore wall and F represents the hypergeometric function. Note that the complete analytical potential model for cylindrical pores is derived from the pair-additive Lennard-Jones (LJ) potential interaction between fluid and wall sites. This kind of surface was called surface I.

For the second surface model, a pore with a hard cylindrical surface decorated by CGs was introduced to investigate adsorption caused solely by the chemical heterogeneity. In this work the CGs are modeled as LJ particles on the interior surface of the cylindrical pore. Two cases were considered here for the arrangement of the CGs. In the first case the CGs were added and fixed in a certain region of the cylindrical surface, i.e., the decorating area. The decorating area here takes the shape of a narrow strip parallel to the axis of the cylindrical pore. In detail, a total of 2400 CGs were randomly added on the decorated areas of the cylindrical pores with a box length of $60\sigma_{f\text{-}f}$. In the second case, the CGs were allowed to rearrange their positions by moving randomly along the interior surfaces of the cylindrical pores according to the Metropolis method. In our simulations, the fluid-fluid and fluid-CG interactions are described by the Lennard-Jones potential between particles i and j:

$$U_{ij} = 4\varepsilon_{ij}[(\sigma_{ij}/r_{ij})^{12} - (\sigma_{ij}/r_{ij})^6]. \quad (2)$$

Here r is the distance between the centers of two interacting sites of types i and j. Other than attractive fluid-CG interaction, the wall is purely repulsive. Note that in our simulation no CG-CG interaction was considered. Instead, a minimum distance between two neighboring CGs was introduced to prevent them from strong overlaps. This kind of surfaces was called surface II in this work.

For the third surface model, a more realistic pore model with both a homogeneous attractive substrate and CGs was used. This kind of surface is in fact a superposition of surfaces I and II, and was called surface III here. Obviously,

adsorption at surfaces I and II is solely caused by the homogeneous substrate and the CGs, respectively, and the values serve as references. While the overall adsorption on surface III results not only from the homogeneous substrate (represented by surface I) and the CGs (represented by surface II), but also from their interplay. Therefore, the interplay between the effects of the homogeneous surfaces and those due to the CGs can be extracted by comparing the three sets of adsorption data obtained from the three kinds of surface.

The parameters used to describe the fluid-fluid interactions are $\sigma_{f\text{-}f}$ and $\varepsilon_{f\text{-}f}$, which are chosen as the LJ parameters for nitrogen molecules in this work (0.375 nm and $95.2k_B$ where k_B is the Boltzmann constant). Fluid-wall interactions are represented by Eqs. (1) and (2), respectively, according to their different origins. Here we fixed $\sigma_{\text{sub-}f}$ (the subscript "sub" denotes the homogeneous substrate) and $\sigma_{\text{CG-}f}$ at 0.265 and 0.2765 nm, respectively, while $\varepsilon_{\text{sub-}f}$ and $\varepsilon_{\text{CG-}f}$ were varied to investigate the cooperative effect. The LJ interactions in this work were cut off at the distance of $4\sigma_{f\text{-}f}$. In the following simulations, we set the temperature to 77 K, the pore diameter to 3.5 nm, the wall thickness of the cylindrical pore to 0.68 nm, and ρ_{solid} to 2.1 in reduced units. In this work, a total of 2400 CGs were added to surfaces II and III on the inner surfaces of the cylindrical pores with the box length of $60\sigma_{f\text{-}f}$. The length of the simulation was longer than 1×10^8. When the acceptance of insertion and deletion moves was very small, the length could reach 5×10^8 for reasonable statistics. A detailed description of the GCMC method is given in our previous work [43]. Note that all the energy parameters hereafter are reduced by $\varepsilon_{f\text{-}f}$.

III. RESULTS AND DISCUSSION

A. Cooperative adsorption

First, we set $\varepsilon_{\text{sub-}f}=1.72$ and $\varepsilon_{\text{CG-}f}=0.4$ to study the adsorption behavior for the three surfaces. Figure 2(a) shows the overall adsorption for surface III, where the amounts of adsorption for surfaces I and II are given as references. The underlying reasons for the fact that capillary condensation occurs earlier for surface III than for surface I are twofold. First, the chemical groups on surface III undoubtedly enhance the adsorption of the first layer, which in turn promotes the nucleation of capillary condensation. Second, the addition of chemical groups on the substrate would result in a deeper potential well in the pore center, which strongly favors capillary condensation, as shown in our previous work [44].

As shown in Fig. 1, the values of adsorption caused by surfaces I and II do not add up to the overall adsorption, indicating the existence of a cooperative effect. The overall adsorption originates from the homogeneous substrate and CGs as well as their cooperative effect. It is the cooperative effect that causes the overall adsorption to exceed the sum of adsorptions caused by surfaces I and II. Here the corresponding adsorption due to the cooperative effect is called the cooperative adsorption.

Although significant difference is observed between the adsorption isotherms for the three surface models, it is hard to recognize the cooperative effect directly from Fig. 2(a). To characterize the cooperative effect, in this work we defined a variable as the ratio of the overall adsorption to the sum of adsorption uptake by the substrate and that by the CGs. The variable is given as follows:

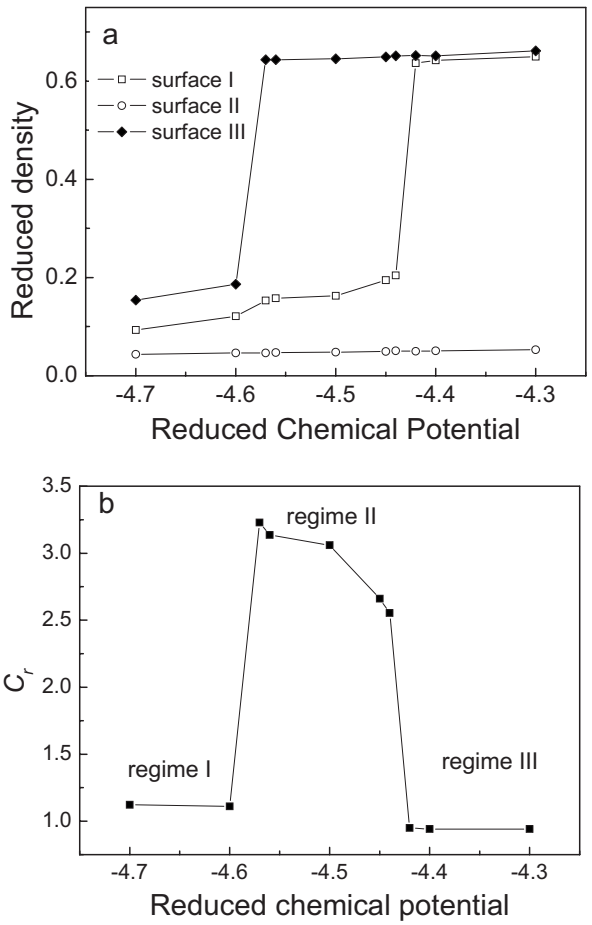

FIG. 2. (a) Adsorption isotherms of nitrogen for three different pore models. The three models are a pore model in which adsorption is caused solely by the homogeneous surfaces (surface I), a pore model in which adsorption is caused solely by CGs (surface II), and a pore model in which both the homogeneous and heterogeneous parts exist (surface III). (b) C_r as a function of the chemical potential. Here C_r was calculated by using Eq. (3) and the data in (a).

$$C_r(\varepsilon_{\text{sub-}f},\varepsilon_{\text{CG-}f})=\frac{\Gamma_{\text{III}}(\varepsilon_{\text{sub-}f},\varepsilon_{\text{CG-}f})}{\Gamma_{\text{I}}(\varepsilon_{\text{sub-}f})+\Gamma_{\text{II}}(\varepsilon_{\text{CG-}f})}, \tag{3}$$

where Γ_{III} represents the overall adsorption for surface III, in which both the CGs and homogeneous substrate are present, while Γ_{II} represents the adsorption uptake for surface II which is caused solely by the CGs and Γ_{I} represents the adsorption uptake for surface I which is caused solely by the homogeneous substrate.

To calculate C_r, three sets of data that appear in the right of Eq. (3) are required. After using Eq. (3), the three curves in Fig. 2(a) assemble to one curve of C_r. As is shown in Fig. 2(b), the curve shows typically three different regions. In the first region, which corresponds to the range of chemical potentials before the capillary condensation of the overall ad-

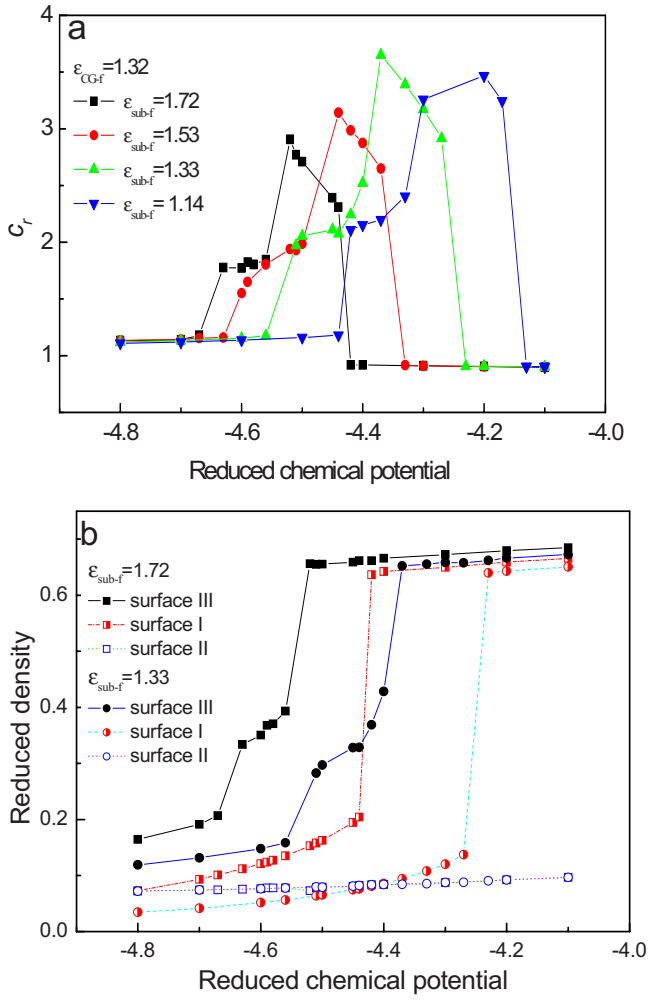

FIG. 3. (Color online) (a) Effects of the fluid-substrate interaction on the cooperative adsorption when $\varepsilon_{CG\text{-}f}$ is set to 1.32. (b) Adsorption isotherms for adsorption caused solely by homogeneous surfaces, that caused solely by CGs, and that for overall adsorption, respectively. $\varepsilon_{CG\text{-}f}$ is set to 1.32, and $\varepsilon_{sub\text{-}f}$ to 1.72 and 1.33.

sorption, C_r is larger than 1. This indicates that the overall adsorption is greater than the sum of the adsorption uptakes caused separately by homogeneity and by CGs. For the second region a significant peak can be found from the curve of C_r. Comparison of Figs. 2(b) and 2(a) shows that the left side of region II corresponds to the capillary condensation for overall adsorption, while its right side corresponds to the capillary condensation for the homogeneous substrate. In this region C_r is much larger than 1, and significant fluctuations were sometimes found. It is the cooperative effects between CGs and the substrate on the adsorption that leads to capillary condensation of the overall adsorption at much lower chemical potential, compared with that for the homogeneous substrate or CGs. In other words, the width of the second region denotes how early the capillary condensation happens due to the cooperative effects, and thus represents cooperative adsorption. Therefore, region II provides information about the cooperative effects between the substrate and CGs on the overall adsorption, and it generally indicates the magnitude of the cooperative effect. From Fig. 2(b) it is found

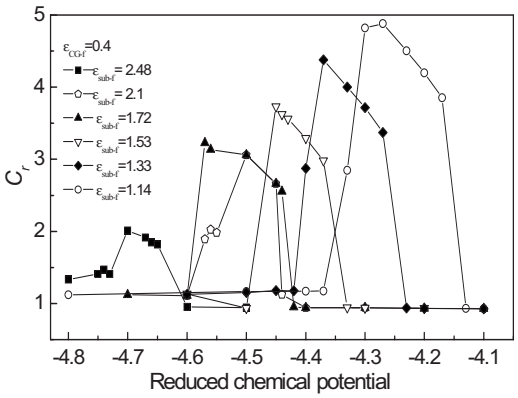

FIG. 4. Effects of the fluid-substrate interaction on the cooperative adsorption when $\varepsilon_{CG\text{-}f}$ is set to 0.4

that C_r is smaller than 1 in the last region because of space restrictions. After capillary condensation for the homogeneous substrate, the space of the pore is so limited that there is no accessible space left to adsorb more molecules, even though CGs are added to promote adsorption. That is to say, in region III, the cooperative effects are suppressed and the overall adsorption is smaller than the sum of that on the homogeneous substrate and that on the CGs.

In order to study the overall adsorption, which originates from the homogeneous substrate and CGs as well as the cooperative effect, the energy parameters describing the fluid-substrate interaction, $\varepsilon_{sub\text{-}f}$, and fluid-CG interaction, $\varepsilon_{CG\text{-}f}$, were varied to study their influence and how they couple. The results are given below.

B. Effects of the homogeneous substrate on cooperative adsorption

To consider the effects of the homogeneous substrate on cooperative adsorption, we decreased $\varepsilon_{sub\text{-}f}$ from 1.72 to 1.14 gradually while $\varepsilon_{CG\text{-}f}$ was kept fixed at 1.32. The values of C_r obtained are shown in Fig. 3 as a function of chemical potential. Similar to the curve for C_r in Fig. 2(b), three regions are found for each set of energy parameters. At lower chemical potential (region I) before capillary condensation of the overall adsorption, C_r is larger than but not far from 1. At much higher chemical potentials (region III) after capillary condensation for surface I, C_r is smaller than 1 due to space restrictions, similar to the results in Fig. 2(b). As for region II, it is found from Fig. 3(a) that, as $\varepsilon_{sub\text{-}f}$ decreases, the location of the second region moves to higher chemical potential. This is because when $\varepsilon_{sub\text{-}f}$ decreases capillary condensation for both surfaces I and III at much higher chemical potentials [44–46], as is shown in Fig. 3(b).

Next, we fixed $\varepsilon_{CG\text{-}f}$ at 0.4, which represents much weaker fluid-CG interaction than that in the case of $\varepsilon_{CG\text{-}f}$ =1.32. The calculated values of C_r as a function of the chemical potential are shown in Fig. 4. Similarly to the results in Fig. 3(a), region II moves to much higher chemical potential as $\varepsilon_{sub\text{-}f}$ decreases. Moreover, Fig. 4 clearly shows a trend for the width of the region to become larger as the energy parameter for the fluid-substrate interaction decreases. In fact, the same trend is also observed in Fig. 3,

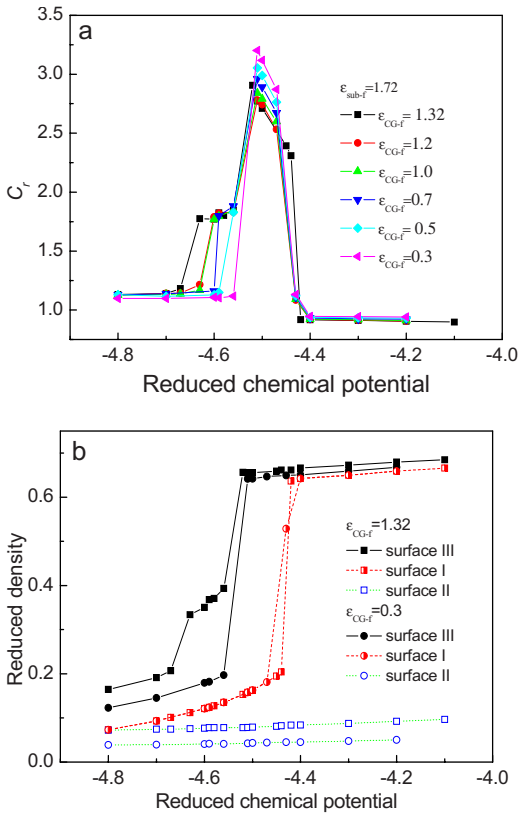

FIG. 5. (Color online) (a) Effects of the fluid-CG interaction on the cooperative adsorption when $\varepsilon_{sub\text{-}f}$ is set to 1.72. (b) Adsorption isotherms for adsorption caused by the homogeneous substrate, that caused by CGs, and the overall adsorption, respectively. $\varepsilon_{sub\text{-}f}$ is set to 1.72, and $\varepsilon_{CG\text{-}f}$ to 1.32 and 0.3, respectively.

although it is not so pronounced. Adsorption isotherms [for example, see Fig. 3(b)] show that for all the cases studied in this section adsorption caused by the homogeneous substrate significantly exceeds that by CGs. This means that for all the cases we studied in this section the overall adsorption is dominated by $\varepsilon_{sub\text{-}f}$, while the effects of CGs are less important. Therefore, it is concluded that when the homogeneous substrate dominates the overall adsorption, the increase of $\varepsilon_{sub\text{-}f}$ leads to a narrower region II, indicating a weaker cooperative effect. It is expected that, if the substrate is attractive enough, all the values of C_r will be close to 1. In this extreme condition, the effects of $\varepsilon_{CG\text{-}f}$ are negligible, and no cooperative adsorption occurs.

In general, when $\varepsilon_{sub\text{-}f}$ dominates overall adsorption, the decrease of the parameter causes capillary condensation of overall adsorption to happen at higher chemical potential, and results in a larger width of region II at the same time.

C. Effects of chemical groups on cooperative adsorption

In this section, we fixed $\varepsilon_{sub\text{-}f}$ at 1.72 and 1.14, and gradually decreased $\varepsilon_{CG\text{-}f}$ from 1.32 to 0.3 to study the effects of the CGs on the overall adsorption and to justify the cooperative effect. The corresponding results are shown in Figs. 5 and 6, respectively. Note that, for all the cases studied here, the homogeneous substrates again dominate the overall adsorption [see, for example, Fig. 5(b)]. The figure also shows that as $\varepsilon_{CG\text{-}f}$ increases from 0.3 to 1.32, capillary condensation for overall adsorption occurs at a lower chemical potential. Hence, the left side of region II moves to a lower chemical potential. And, because $\varepsilon_{sub\text{-}f}$ is fixed, capillary condensation for the homogenous substrate occurs at the same chemical potential; thus the right side of the region is fixed. This is why the width of region II increases with $\varepsilon_{CG\text{-}f}$. Although they represent different $\varepsilon_{sub\text{-}f}$, Figs. 5 and 6 show the same trend. The trend is that the increase of $\varepsilon_{CG\text{-}f}$, like the decrease of $\varepsilon_{sub\text{-}f}$ discussed in the previous section, results in a wider region II; on the other hand, the capillary condensation for the overall adsorption happens at a lower chemical potential.

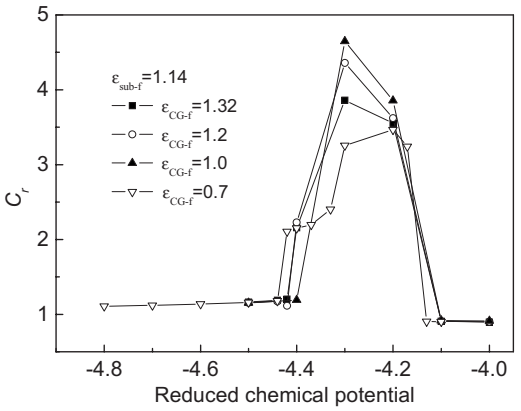

FIG. 6. Effects of the fluid-CG interaction on the cooperative adsorption when $\varepsilon_{sub\text{-}f}$ is set to 1.14.

In summary, when $\varepsilon_{sub\text{-}f}$ dominates overall adsorption, the decrease of the parameter leads capillary condensation to happen at a higher chemical potential, and at the same time results in a larger width of region II, which indicates a strong cooperative effect. Alternatively, the increase of $\varepsilon_{CG\text{-}f}$ also results in a wider region II, but the capillary condensation for the overall adsorption happens at a lower chemical potential.

D. Effects of distribution of chemical groups

To investigate the effects of the CG distribution on the overall adsorption, and to obtain the distribution of CGs, where the CGs dominate the overall adsorption, a design-test method (see, for example, Refs. [47–49]) is generalized and used in this work. This method is often used to design optimum surfaces for recognizing specific monomer sequences in copolymers or proteins. A simulation with this method is split into two steps: a design step and a test step. In the design step, the heterogeneous surface is trained to recognize the monomer sequence by adsorption of a bulk polymer (protein). In the test step, the designed surface is tested by observing whether the surface recognizes and selectively adsorbs the copolymers or proteins with the right sequence. Inspired by those works, we used this method to optimize the distribution of CGs, rather than monomer sequences as in its conventional applications. In this work, the distribution of CGs on a homogeneous substrate was first trained in the design step to make the adsorption better, and then the de-

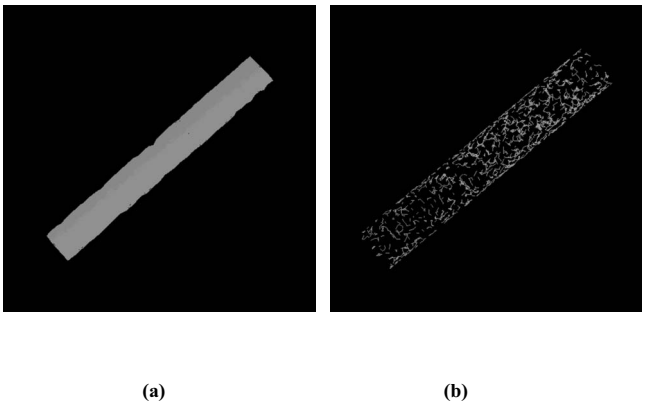

FIG. 7. Comparison of the snapshots of CG distribution for (a) the case where CGs were added and fixed on certain areas of the cylindrical surface and (b) the case that the distribution of CGs is trained by the design step.

signed distribution of CGs was checked by the test step.

The design step aims at designing an ensemble of CG distributions to give optimized adsorption. Therefore, a heterogeneous surface is designed in target configurations, for which a low-energy state is expected. Different from the cases where the CGs were fixed on the pore surface during GCMC simulations, in the designed step an *NVT* MC method was used and the CGs were allowed to move randomly along the surface. Therefore, in addition to the type of moves that move fluid molecules randomly, the movement of CGs along the surface was also performed to rearrange their position, according to the Metropolis method. No CG-CG interaction was considered in the work. However, a minimal distance of 0.5 for the neighboring CGs was adopted to prevent them from strong overlaps. At the end of the step, an ensemble of target configurations was obtained. A typical snapshot is shown in Fig. 7(b). In order to quantify the distribution of CGs on the designed surfaces, we use an order parameter (OP) defined as

$$\sum^{N_{\text{pair}}} (r_{ij})^2 / N_{\text{pair}} \tag{4}$$

where N_{pair} is the total number of pairs of CGs and r_{ij} is the distance between two CGs. Figure 8 shows the evolution of the order parameter during the design step. In general, the order parameter is a good description of the aggregation of CGs, and the design method to optimize the distribution of CGs is feasible and effective.

The test step proceeds in the following manner. After the design step, one of the obtained distributions of CGs [see Fig. 7(b)] was used as the input of the test step. Then, in this step, the GCMC method with that CG distribution was applied to calculate adsorption isotherms. First we set $\varepsilon_{\text{CG-}f}$ =0.4 and then increase $\varepsilon_{\text{CG-}f}$ to 0.8, 1.2, and 1.6, while $\varepsilon_{\text{sub-}f}$ was fixed at 1.14. We compared the values of C_r for the unoptimized heterogeneous surface (in which CGs were fixed on certain regions of the pore wall) with those for the designed heterogeneous surface in Fig. 9(a) at $\varepsilon_{\text{CG-}f}$=0.4. Obviously, in the case where the distribution of CGs was optimized, region II of C_r is much wider. Because both the

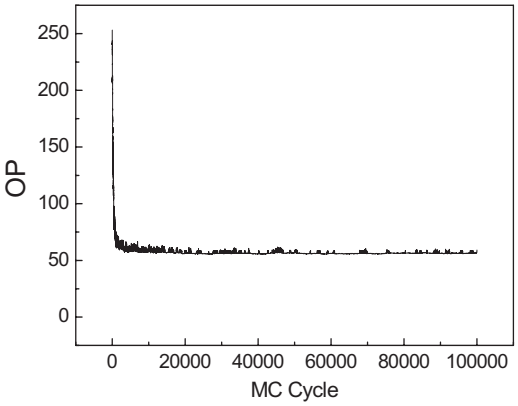

FIG. 8. Evolution of the order parameter during the design step.

shape and the position of region II for the optimized surface are different from those without optimization, a different mechanism for the cooperative adsorption is expected for the optimized surface. Adsorption isotherms [see Fig. 9(b)] show that the capillary condensation for the designed surface occurred in a position with a substantially lower chemical potential. This indicates that the distribution of CGs affects the cooperative adsorption significantly.

Moreover, for the designed surface the variation of C_r with different $\varepsilon_{\text{CG-}f}$ (see Fig. 10) shows a different trend from that for surfaces without optimization. When no opti-

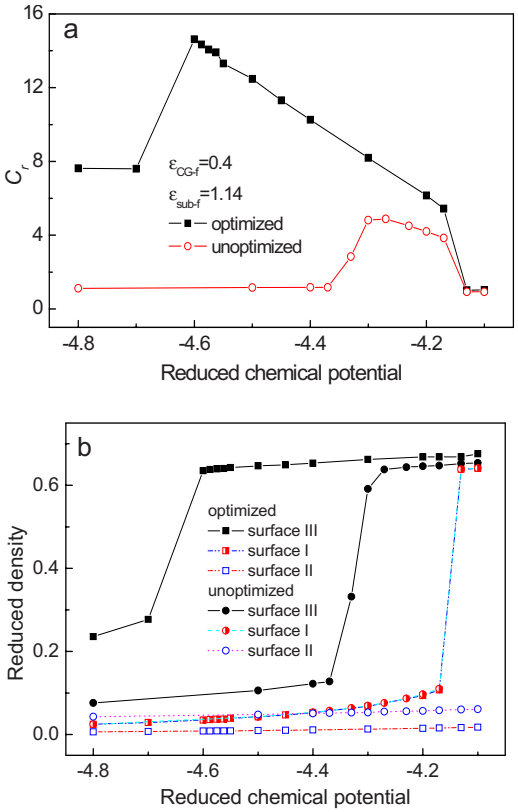

FIG. 9. (Color online) (a) Comparison of C_r for the trained surface and the untrained surface. $\varepsilon_{\text{sub-}f}$ is set to 1.14, and $\varepsilon_{\text{CG-}f}$ is set to 0.4. (b) The corresponding adsorption isotherms for the two different surfaces.

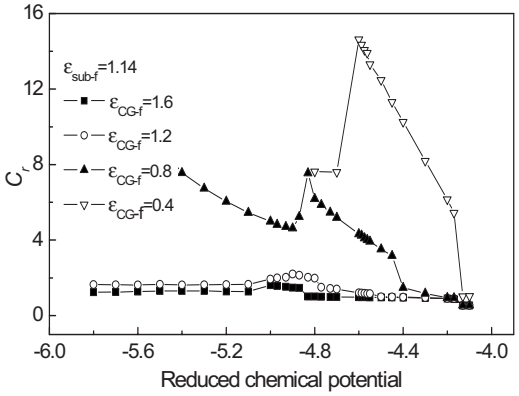

FIG. 10. Effects of the fluid-CG interaction on the cooperative adsorption when $\varepsilon_{\text{sub-}f}$ is set to 1.14.

mization of the distribution of CGs was performed as is done in the section above, the width of region II becomes larger as $\varepsilon_{\text{CG-}f}$ increases. But for the optimized surface, the trend is just the opposite: the width of region II becomes smaller as $\varepsilon_{\text{CG-}f}$ increases from 0.4 to 0.8, 1.2, and 1.6. The reason for this difference can be interpreted from Fig. 11. Figure 11(a) and 11(b) show the adsorption isotherms for $\varepsilon_{\text{CG-}f}=1.6$ and 0.8, respectively. First, after the CG distribution is optimized, adsorption caused solely by the CGs is substantially enhanced, and the corresponding chemical potential for capillary condensation occurs nearby [see Fig. 11(a)], or even

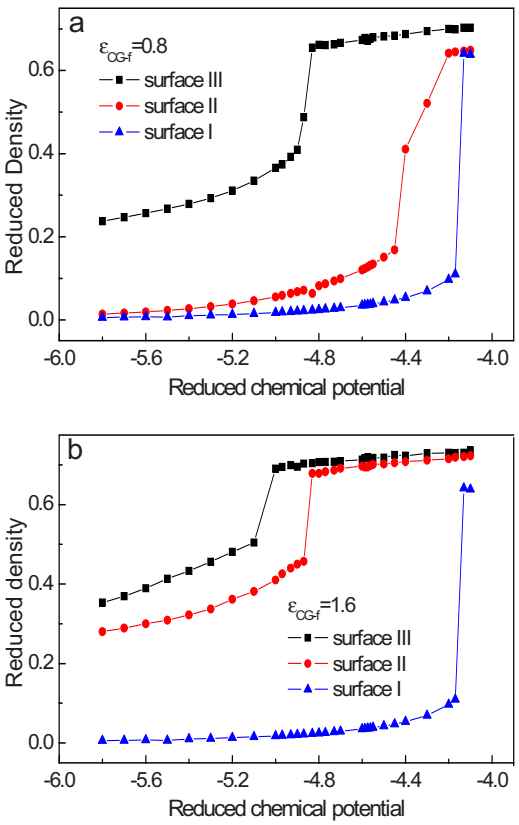

FIG. 11. (Color online) (a) Adsorption isotherms for the designed heterogeneous surface when (a) $\varepsilon_{\text{sub-}f}$ is set to 1.14 and $\varepsilon_{\text{CG-}f}$ to 0.8 and (b) $\varepsilon_{\text{sub-}f}$ is set to 1.14 and $\varepsilon_{\text{CG-}f}$ is set to 1.6.

lower than that caused by the homogeneous surface [see Fig. 11(b)]. Therefore, the overall adsorption in this case is no longer dominated just by $\varepsilon_{\text{sub-}f}$, as in the previous sections, but by $\varepsilon_{\text{CG-}f}$ instead (for example, in the cases $\varepsilon_{\text{CG-}f}=1.2$ and 1.6), or at least the two factors are roughly of the same importance (in the cases $\varepsilon_{\text{CG-}f}=0.4$ and 0.8). Figure 10 shows that as $\varepsilon_{\text{CG-}f}$ increases from 0.8 to 1.6, the maximal value of C_r in the region II decreases from 12 to 2. Thus, it is concluded that, if $\varepsilon_{\text{CG-}f}$ dominates the overall adsorption, the increase of $\varepsilon_{\text{CG-}f}$ or alternatively the decrease of $\varepsilon_{\text{sub-}f}$ will make the cooperative effect weaker.

IV. CONCLUSIONS

The effects of the surface heterogeneity of pore media on the adsorption behavior is of both fundamental and practical importance. In most cases, the heterogeneity of realistic surfaces can reasonably be modeled as a combination of a homogeneous substrate and chemical heterogeneities decorating it. In this work we studied the interplay of physical adsorption due to a homogeneous substrate and its heterogeneity. Heterogeneity here is represented by the number of chemical groups decorating the homogeneous substrate. The adsorption caused by the homogeneous substrate only and that by CGs do not add up to the overall adsorption, indicating the existence of a cooperative effect. The cooperative effect is the source of cooperative adsorption. In this work the cooperative effect is characterized by the ratio of the overall adsorption to the sum of that by the substrate and that by CGs.

We show here that the cooperative adsorption does not monotonically depend on the substrate or the CGs. The different origins play different roles depending on which one dominates the overall adsorption. In general, when the fluid-substrate interaction $\varepsilon_{\text{sub-}f}$ dominates the overall adsorption, the decrease of the parameter leads the capillary condensation to happen at higher chemical potential, and results in a wider region II at the same time. Therefore, the cooperative effect becomes stronger and cooperative adsorption is enhanced. On the other hand, the increase of the fluid-CG interaction $\varepsilon_{\text{CG-}f}$ also results in a wider region II and enhances the cooperative effect, but causes capillary condensation to happen at a lower chemical potential. In contrast, if the effects of $\varepsilon_{\text{CG-}f}$ dominate the overall adsorption, the decrease of $\varepsilon_{\text{CG-}f}$, or alternatively the increase of $\varepsilon_{\text{sub-}f}$, leads to a stronger cooperative effect and enhances the cooperative adsorption. The strongest cooperative adsorption occurs when the two factors are roughly of the same importance.

To investigate the effects of the distribution of CGs on the cooperative adsorption, a design-test method was generalized and used in this work. A simulation with this method was split into two steps: a design step and a test step. In this work, the distribution of CGs on a substrate was first trained in the design step to make adsorption better. In order to give optimized adsorption, in the design step the CGs were allowed to move randomly along the surface to design an ensemble of heterogeneous surfaces. Then, the designed distribution of CGs was checked by the test step. The simulation

results show that the effect of the distribution of CGs on the cooperative adsorption is significant. For example, in some cases, such as $\varepsilon_{CG\text{-}f}=1.2$ and 1.6 when $\varepsilon_{sub\text{-}f}$ is fixed at 1.14, the overall adsorption is dominated by $\varepsilon_{sub\text{-}f}$ before the surfaces were trained. However, after the heterogeneous surfaces were trained, the overall adsorption is dominated by $\varepsilon_{CG\text{-}f}$ instead.

ACKNOWLEDGMENTS

The work is supported by the National Natural Science Foundation of China (Grant No. 20736005). X.Z. acknowledges the support of the Research Foundation for Young Researchers of BUCT. Generous allocations of computer time by the "Chemical Grid Project" of BUCT and the Supercomputing Center, CNIC, CAS are acknowledged.

[1] Y. Wan, H. Yang, and D. Zhao, Acc. Chem. Res. **39**, 423 (2006).
[2] A. P. Wight and M. E. Davis, Chem. Rev. **102**, 3589 (2002).
[3] J. E. Lim, C. B. Shim, J. M. Kim, B. Y. Lee, and J. E. Yie, Angew. Chem. Int. Ed. **43**, 3839 (2004).
[4] C. Liang, Z. Li, and S. Dai, Angew. Chem., Int. Ed. **47**, 3696 (2008).
[5] X. Chen and S. S. Mao, Chem. Rev. **107**, 2891 (2007).
[6] M. Jaroniec, C. P. Jaroniec, M. Kruk, and R. Ryoo, Adsorption **5**, 313 (1999).
[7] L. D. Gelb, K. E. Gubbins, R. Radhakrishnan, and M. Sliwinska-Bartkowiak, Rep. Prog. Phys. **62**, 1573 (1999).
[8] M. Schoen, Phys. Chem. Chem. Phys. **10**, 223 (2008).
[9] R. Evans, U. Marini Bettolo Marconi, and P. Tarazona, J. Chem. Soc., Faraday Trans. 2 **82**, 1763 (1986).
[10] R. Evans, U. Marini Bettolo Marconi, and P. Tarazona, J. Chem. Phys. **84**, 2376 (1986).
[11] J. P. R. B. Walton and N. Quirke, Mol. Simul. **2**, 361 (1989).
[12] E. Pitard, M. L. Rosinberg, and G. Tarjus, Mol. Simul. **17**, 399 (1996).
[13] P. Röcken, A. Somoza, and P. Tarazona, J. Chem. Phys. **108**, 8689 (1998).
[14] E. Kierlik, P. A. Monson, M. L. Rosinberg, L. Sarkisov, and G. Tarjus, Phys. Rev. Lett. **87**, 055701 (2001).
[15] L. Sarkisov and P. A. Monson, Phys. Rev. E **65**, 011202 (2001).
[16] A. V. Neimark, P. I. Ravikovitch, and A. Vishnyakov, Phys. Rev. E **65**, 031505 (2002).
[17] K. Bucior, A. Patrykiejew, O. Pizio, and S. Sokołowski, J. Colloid Interface Sci. **259**, 209 (2003).
[18] F. Detcheverry, E. Kierlik, M. L. Rosinberg, and G. Tarjus, Langmuir **20**, 8006 (2004).
[19] F. Porcheron, P. A. Monson, and M. Thommes, Langmuir **20**, 6482 (2004).
[20] B. Libby and P. A. Monson, Langmuir **20**, 4289 (2004).
[21] P. Röcken and P. Tarazona, J. Chem. Phys. **105**, 2034 (1996).
[22] R. J.-M. Pellenq and P. E. Levitz, Mol. Phys. **100**, 2059 (2002).
[23] R. Van Slooten, M. J. Bojan, and W. A. Steele, Langmuir **10**, 542 (1994).
[24] M. W. Maddox, D. Ulberg, and K. E. Gubbins, Fluid Phase Equilib. **104**, 145 (1995).
[25] E. A. Müller, L. F. Rull, L. F. Vega, and K. E. Gubbins, J. Phys. Chem. **100**, 1189 (1996).
[26] M. Schoen and D. J. Diestler, Chem. Phys. Lett. **270**, 339 (1997).
[27] M. Schoen and D. J. Diestler, Phys. Rev. E **56**, 4427 (1997).
[28] P. Röcken, A. Somoza, P. Tarazona, and G. H. Findenegg, J. Chem. Phys. **108**, 8689 (1998).
[29] A. Vishnyakov, E. M. Piotrovskaya, and E. N. Brodskaya, Adsorption **4**, 207 (1998.).
[30] E. A. Müller and K. E. Gubbins, Carbon **36**, 1433 (1998).
[31] M. Alvarez, D. Levesque, and J.-J. Weis, Phys. Rev. E **60**, 5495 (1999).
[32] C. McCallum, T. J. Bandosz, S. C. McGrother, E. A. Müller, and K. E. Gubbins, Langmuir **15**, 533 (1999).
[33] H. Bock and M. Schoen, Phys. Rev. E **59**, 4122 (1999).
[34] J. K. Brennan and W. Dong, J. Chem. Phys. **116**, 8948 (2002).
[35] J. K. Brennan and W. Dong, Phys. Rev. E **67**, 031503 (2003).
[36] J. Puibasset and R. J.-M. Pellenq, J. Chem. Phys. **118**, 5613 (2003).
[37] H.-J. Woo, F. Porcheron, and P. A. Monson, Langmuir **20**, 4743 (2004).
[38] B. Coasne and R. J.-M. Pellenq, J. Chem. Phys. **120**, 2913 (2004).
[39] J. Puibasset, J. Phys. Chem. B **109**, 8185 (2005).
[40] J. Puibasset, J. Phys. Chem. B **109**, 4700 (2005).
[41] J. Puibasset, J. Chem. Phys. **122**, 134710 (2005).
[42] G. R. Birkett and D. D. Do, Langmuir **22**, 9976 (2006).
[43] X. Zhang, W. Wang, and G. Jiang, Fluid Phase Equilib. **218**, 239 (2004).
[44] X. Zhang, D. Cao, and W. Wang, J. Chem. Phys. **119**, 12586 (2003).
[45] X. Zhang and W. Wang, Phys. Rev. E **74**, 062601 (2006).
[46] X. Zhang, D. Cao, and W. Wang, J. Colloid Interface Sci. **308**, 49 (2007).
[47] A. Jayaraman, C. K. Hall, and J. Genzer, Phys. Rev. Lett. **94**, 078103 (2005).
[48] I. Coluzza and D. Frenkel, Phys. Rev. E **70**, 051917 (2004).
[49] A. J. Golumbfskie, V. S. Pande, and A. K. Chakraborty, Proc. Natl. Acad. Sci. U.S.A. **96**, 11707 (1999).